Supplementary Information

Zinc finger-inspired peptide-metal-phenolic nanointerface enhances bone-implant integration under bacterial infection microenvironment through immune modulation and osteogenesis promotion

Lin Xu, Jie Fang, Jiezhou Pan, Hexu Qi, Yun Yin, Yunxiang He, Xueqi Gan, Yifei Li[*], *Yu Li*[**], *Junling Guo*[***]

Table of Contents

S1. Supplementary methods

1. Materials characterization of ABL@ZnTAnanointerface

1.1 Release, loading efficiency, and adhesion behavior

We studied the impact of the assembly strategy on the structural stability of the ABL peptide using Circular Dichroism. The native ABL peptide solution and the above TA-ABL coating with the same concentration of ABL were measured in Milli-Q water. Besides, the ABL release profiles of various coatings were evaluated in vitro by immersing the coated Ti disks in PBS, and the supernatant was collected daily for 6 d to measure the peptide concentration. As no commercial ELISA kit is available for ABL peptide, FITC-labeled ABL was used instead. The fluorescence intensity was measured using an automatic microplate reader (Thermo 3001, USA).

The loading efficiency of ABL@ZnTA coating is determined by calculating the drug load per unit area. For the loading efficiency of ABL, Ti substrates coated with FITC-labeled ABL-TA were eluted in 100 mM urea, 100 mM Tween 20, or 100 mM NaCl solution to determine total content and the interaction strength of ionic interactions, hydrogen bonding, and hydrophobic interactions, respectively. The fluorescence intensity was measured using an automatic microplate reader (Thermo 3001, USA). Besides, the coated titanium plates are thoroughly eluted with a 0.1mmol/L HCl solution, and the content of TA is measured by high-performance liquid chromatography (HPLC, Thermo ICAP PRO, USA), while the Zn^{2+} content is measured by inductively coupled plasma optical emission spectrometry (ICP-OES, Thermo ICAP PRO, USA). Coated Ti substrates were soaked in PBS for 7 and 21 d to further verify the long-term adhesion of the phenolic-peptide network. The surface topography of the Ti substrates was analyzed using SEM. The mechanical properties of various coatings were evaluated by a nanoindenter instrument (Anton Paar, UNHT, Austria). Young's modulus and hardness were calculated from force versus indentation depth curves.

1.2. Molecular dynamics simulations

The ABL was constructed into an α-helix model by referencing the structure retrieved from the PDB database. After the receptor ABL was modeled, a molecular dynamics simulation of 10 ns was carried out separately to show its natural conformation in an aqueous solution. The conformation of the simulated final moment and the ligand TA were used for molecular docking with the Ledock program. The global molecular docking method was adopted due to the unknown binding site of the receptor and ligand. The initial simulation boxes had dimensions of 9 nm × 6 nm × 6 nm. A minimum RMSD of 0.5Å was set for docking conformation, and only 5 conformations were allowed.

Molecular dynamics simulation was performed using the docking conformation with the highest score as the starting structure. The docking complex was solvated and had its ionic charge neutralized. Following energy minimization and pre-balance, a 200 ns formal simulation was conducted. Parameters were then extracted from the simulation locus of the acceptor-ligand complex using the analysis instructions inherent in Gromacs. The free binding energy of the complex was calculated using gmx MMPBSA, and visualization was performed using Pymol.

2. In vitro experiment

2.1. Compatibility evaluation

The cytoskeleton was observed by marking F-actin with FITC-phalloidin (Solarbio Corporation, Beijing, China). After 2 d of incubation, the cells were fixed with 4 % PFA for 20 min and permeabilized with 0.1 % (v/v) Triton X-100 (Sigma, USA) in PBS for 15 min. The cell cytoskeleton was stained using FITC-phalloidin (Sigma), and the nuclei were stained using 4',6-diamidino-2-phenylindole (DAPI; Solarbio Corporation) to stain cellular actin filaments and nuclei respectively. Fluorescent imaging of cells was captured using CLSM (Olympus, FV10-ASW).

Additionally, the cell-attached samples were observed using SEM. Briefly, cells were fixed with 2.5 % glutaraldehyde for 2 h at room temperature. After that, samples were dehydrated in a sequential gradient ethanol (25, 50, 75, 85, 95, and 100 %) for 30 min sequentially. Subsequently, the cells were dried through critical point drying, sprayed with gold, and observed using SEM.

Live/dead staining (Beyotime, Shanghai, China) was performed to assess cell viability on substrates qualitatively. MC3T3 cells were inoculated onto each sample in a 24-well plate for 2 d. Next, a working solution of Calcein acetoxymethyl ester (Calcein-AM, green fluorescence; Sigma, USA) and Propidium iodide (PI, red fluorescence; Sigma, USA) diluted at 1:1000 in serum-free medium was added to each sample and incubated for 30 min. After gently rinsing with PBS, cells on the samples were captured using CLSM (Olympus, FV10-ASW). The live-to-dead cell numbers ratio was detected and calculated using ImageJ software (NIH, Bethesda, MD, USA) based on at least 3 random fields.

In addition, a Cell Viability Assay by culturing cells for 2 and 3 d using a CCK-8 kit (Dojindo, Japan). At each checkpoint, the media was replaced with a 300 μL mixed solution (CCK-8 working solution) and was coincubated at 37 °C for 1 h. Then, 100 μL of the supernatants were transferred into a new 96-well plate separately, and the absorbance was measured at 450 nm using a microplate reader (Molecular Devices, Sunnyvale, CA).

2.2. The immuno-modulatory properties

The cells were treated with 1 μg/mL LPS to induce inflammatory microenvironment. The expression of biomarkers was examined via qRT-PCR assay after 2 d (n = 3), including M1 marker nitric oxide synthase (*iNOS)*, pro-inflammatory cytokines (*TNF-α*, *IL-1β*), pro-healing cytokines (*IL-4*, *IL-10*), and *TGF-β* secreted by the polarized macrophages. Total RNA was extracted using an mRNA rapid extraction kit (Yishan, Shanghai, China) according to the manufacturer's protocol. Reverse transcription was done for the extracted RNA using PrimeScript TM RT reagent Kit with gDNA Eraser (Takara, Japan). qRT-PCR was performed using a SYBER Green PCR kit (Applied Biosystems, Foster City, CA, USA) and StepOne Real-Time PCR System (Applied Biosystems). The primer sequences are listed in Table S1. All values were normalized to glyceraldehyde-3-phosphate dehydrogenase and analyzed using the ΔΔCt method. The experiments were performed in triplicate.

Besides, macrophage phenotypic polarization was conducted in vitro through immunofluorescence staining. After 2 d, the RAW264.7 cells on coated substrates were washed by PBS and fixed in 4 % paraformaldehyde for 5 min, permeabilized in PBS, supplemented with 0.1 % Triton X-100 for 15 min, and then blocked with 3 % BSA at room temperature for 40 min and later incubated overnight at 4 °C in a humidified chamber with rabbit anti-mouse iNOS (1:200 in dilution; Abcam Biochemicals, UK) and CD206 (1:200 in dilution; Abcam Biochemicals, UK). The cells were incubated with goat anti-rabbit secondary antibody (1:200)

(ZSGB-Bio, China) and phalloidine (1:1000) for 1 h, then washed twice with PBS and incubated with DAPI for 10 min. The cells were then washed 3 times and analyzed using a Leica fluorescence microscope (Olympus, Japan).

2.3. Anti-oxidative and ROS scavenging capacity

Ti disks were modified with functionalized coatings containing different concentrations of loaded drugs. Briefly, the coating mixture containing 50, 100, 200, 500, and 1000 μL ABL were regarded as TA-ABL 50, 100, 200, 500, and 1000. Later, the substrates decorated with Zn^{II} in the same ratio were regarded as co-50, 100, 200, 500, and 1000.

Cell viability tests were conducted to investigate the protective capability of phenolic-peptide functionalized coatings of varying concentrations in a ROS-excess microenvironment. RAW264.7 cells were seeded at a density of 2×10^4 cells per well onto the substrates above and cultured overnight. The cells were then stimulated with H_2O_2 (200 μM) for 12 h to induce excess ROS. The CCK-8 procedure was conducted according to the previous method, and the optimal formula of ABL@ZnTA 100 was determined and used for the subsequent experiment.

Intracellular ROS was identified using the fluorescent probes DCFH-DA (Sigma, USA), CellTracker Red (Molecular Probes, Thermo, USA), and CellRox Green (Molecular Probes, Thermo, USA). RAW264.7 cells were seeded onto substrates with various coatings (10^4/well). To determine ROS levels, the cells were stimulated with H_2O_2 (200 μM) for 2 h, and the cell medium was then replaced with DCFH-DA or above probes (diluted 1:1000) and incubated for 30 min at 37 ℃ in the dark. Fluorescence microscopy images were collected using a Leica imaging system, and semi-quantitative analysis was conducted using ImageJ software.

The microenvironmental ROS scavenging capacity was evaluated using the Total Antioxidant Capacity Assay Kit (Beyotime, Beijing, China). Briefly, Ti substrates with various coatings were soaked in PBS. After 1 d, 200 mL of ABTS working solution was added to a 96-well plate and mixed thoroughly. The 96-well plate was kept in the dark at 25 ºC for 30 min. The absorbance of the ABTS solution was measured at 734 nm using a microplate reader. Trolox was used as a reference antioxidant. The antioxidant capacity of the different coatings was expressed relative to Trolox for convenient comparison.

2.4. Osteogenic potential

MC3T3 cells (1×10^4 cells per well) were seeded onto various substrates in a 24-well plate. The osteogenic potential was evaluated under inflammatory or excessive oxidative stress conditions. To simulate the in vitro inflammatory environment, LPS was added to stimulate the inflammatory response of MC3T3 cells. Once the cell culture reached 80−90 % confluence, the growth media was replaced with osteogenic differentiation media. This media consisted of DMEM supplemented with 100×10^{-9} m dexamethasone (Sigma), 50 μg/mL ascorbic acid (Sigma), and 10×10^{-3} m glycerophosphate (Sigma). The media was updated every 2−3 days. To further evaluate the effects of osteo-immunomodulation and antioxidation of phenolic-peptide coating, MC3T3 cells were seeded in a culture plate and incubated in macrophage-conditioned medium (mixing fresh DMEM and the supernatant of the macrophages culture medium at a volume ratio 1:1). The culture medium was acquired by incubating macrophages on different coated Ti for 2 d stimulated by H_2O_2.

The expression of bone formation-related genes, including *RUNX 2*, *ALP*, *COL 1*, and *OCN*, and the antioxidant-related gene, superoxide dismutase 1 (*SOD 1*), were assessed using qRT-PCR. The methodology used for qRT-PCR was previously described in the immuno-

modulatory effect. The primer sequences used are listed in Table S1. Additionally, pre-osteoblasts were subjected to osteogenic differentiation for 7 and 14 d, and ALP staining was performed. The samples were rinsed with PBS and fixed with 4 % PFA for 30 min at 4 °C. Subsequently, a BCIP/NBT ALP color development kit (Beyotime, Beijing, China) was used to stain the samples according to the manufacturer's protocol. The cells were then washed with ultra-pure water, and the stained images were captured using a stereo microscopes (Olympus, Japan). For the calcium nodule staining experiment, pre-osteoblasts were induced for 14 and 21 d for osteogenic differentiation, and ARS staining was performed. The cells were fixed with 4 % PFA for 15 min and stained with 1 % Alizarin Red S (pH 4.2, Solarbio, Beijing, China) for 5 min. The mineralized matrix was stained dark red. Images were captured using Stereo Microscopes (Olympus, Japan). The elution solution (phosphate buffer containing 10 % cetylpyridinium chloride, pH=7) was used for semi-quantitative analysis and the absorbance value at 562 nm was detected by a multifunctional enzyme marker.

To further evaluate the effect of in vitro mineralization, samples were soaked in simulated body fluid for 3 and 40 d. The surface morphology of the mineralized product was observed. Briefly, the samples were gently washed with Milli-Q water and then dried using critical point drying. Afterward, they were sprayed with gold and observed using SEM.

3. In vivo experiment

The sample size was calculated using power analysis based on the estimated effect size reported in a previous study ($\alpha = 0.05$, $1 - \beta = 0.90$, and effect size = 0.8) [1]. A minimum of 4 rats was required in each group at each time point.

3.1. Evaluation of immune response

Three days after surgery, the rats were sacrificed by intraperitoneal injection of pentobarbital in overdose, and blood was collected from the carotid artery to measure the level of the inflammatory factor TNF-α using an ELISA kit (Solarbio Corporation, Beijing, China). The femur condyles with implants were dissociated, fixed with 4 % paraformaldehyde overnight, and decalcified in 10 % ethylene diamine tetraacetic acid for 6 weeks. The implants were removed after careful dissection of the femur condyles. The tissue gradient was then dehydrated and embedded in paraffin. Horizontal sections, 5-μm thick, were made perpendicular to the implant cross-section. Hematoxylin and eosin (H&E) staining was used to observe the early bone quality and determine morphological conditions. The sections were further processed for IHC staining and analysis. The sections were incubated with primary antibodies against iNOS and CD206 (Abcam, MA, USA) at 4 °C overnight. Subsequently, the sections were incubated with goat anti-rabbit secondary antibody (1:400 in dilution; ZSGB-Bio, Beijing, China) conjugated to horseradish peroxidase for 2 h. Immunoreactivity was visualized using 3,3-diaminobenzidine (Zhongshan, China) for 3–5 min at room temperature. Finally, the slice was imaged using a fully electric automatic microscope (Nikon Eclipse, Japan). For semi-quantitative analysis, the mean density of each section was calculated as the ratio of integrated optical density to the area around the implant using Image-Pro Plus 6.0 (Media Cybernetics, Inc., USA). Three visual fields were uniformly imaged from each region, and the average value was taken as the result of each sample.

3.2. Biomechanical test and bone-to-implant contact

After 28 d post-surgery, bone specimens with implants were harvested. Biomechanical push-out testing was performed to quantify osseointegration for various implants. The push-out tests were conducted using a Universal Mechanical Tester (Instron 8874, Norwood, USA) by applying an axial compression load to the implant at a loading rate of 5.0 mm/min until the bone-implant interface was destroyed. The maximum push-out load was considered as the failure load, and the load-displacement curves were recorded. Additionally, the implants detached from the femur bone were analyzed using SEM and EDS to assess the hydroxyapatite deposits around them. The evaluation procedure is identical to that of cells in the Cytocompatibility evaluation.

The bone specimens were dehydrated in a graded ethanol series (70−100 %) and then embedded in a methyl methacrylate solution and polymerized at 37 °C for a week. Thin sections, 5 μm in thickness, were prepared using a microtome (Leica Microtome, Germany) perpendicular to the implant. The tissue response and bone integration with the implanted materials were assessed using Methylene blue magenta staining.

3.3. Micro-CT analysis

The femoral metaphysis of the femurs with implants was scanned using Micro-CT (SCANCO VivaCT80, Switzerland) with an isotropic voxel size of 15 μm. The energy setting of 70 kVp and an integration time of 300 ms were used. The raw images were reconstructed into serial cross-sections, and femoral histomorphometric parameters were analyzed using SCANCO Medical Evaluation and Visualizer software. The volume of interest (VOI) was defined as a hollow cylinder surrounding the bone marrow, including the 100 μm ring area extending from the implant periphery. Within the VOI, we calculated trabecular number (Tb.N), trabecular thickness (Tb.Th), trabecular separation (Tb.Sp), and bone volume fraction (BV/TV).

3.4. Histomorphometry

After Micro-CT analysis, the samples underwent a 6-week decalcification process and were sectioned using the same procedure as the 3-day histomorphometry. H&E staining was used to observe the morphological conditions of early bone quality. Masson's trichrome staining was performed to evaluate new bone formation, and the ratio of new to old bone area was calculated. IHC of COL 1 (1:200 in dilution; Abcam Biochemicals, UK) was used to illustrate the bone formation around the implant, and the mean density of the positive area was measured for semi-quantitative analysis.

Osteoclasts were also analyzed through enzyme histochemistry in decalcified sections using a TRAP staining kit (Solarbio Corporation, Beijing, China). The area of peri-implant and nearby periosteum were selected as the region of interest. TRAP-positive multinucleated osteoclasts were counted on 3 sections for each specimen, and the mean value and standard deviation for each experimental group were presented.

Supplementary table

Table S1. The primer sequences for qRT-PCR.

Name	Primer Sequence (5' to 3')	Primer Sequence (3' to 5')
iNOS	CACCAAGCTGAACTTGAGCG	CGTGGCTTTGGGCTCCTC
TNF-α	GTGCCAGCCGATGGGTTGTAC	TGACGGCAGAGAGGAGGTTGAC
IL-1β	ACGGACCCCAAAAGATGAAG	TTCTCCACAGCCACAATGAG
IL-4	GGTCTCAACCCCCAGCTAGT	GCCGATGATCTCTCTCAAGTGAT
IL-10	AGCCGGGAAGACAATAACTG	GGAGTCGGTTAGCAGTATGTTG
TGF-β	CCACCTGCAAGACCATCGAC	CTGGCGAGCCTTAGTTTGGAC
RUNX 2	ATGCTTCATTCGCCTCACAAA	GCACTCACTGACTCGGTTGG
ALP	GGAATACGAACTGGATGAGAAGG	GGTTCCAGACATAGTGGGAATG
COL 1	GCTCCTCTTAGGGGCCACT	ATTGGGGACCCTTAGGCCAT
OCN	CACCTAGCAGACACCATGAG	GTTCACTACCTTATTGCCCTCC
SOD 1	ATGGCGATGAAAGCGGTGT	CCTTGTGTATTGTCCCCATACTG
GAPDH	TATGACTCTACCC ACGGCAAGT	ATACTCAGCACCAGCATCACC

Supplementary figures

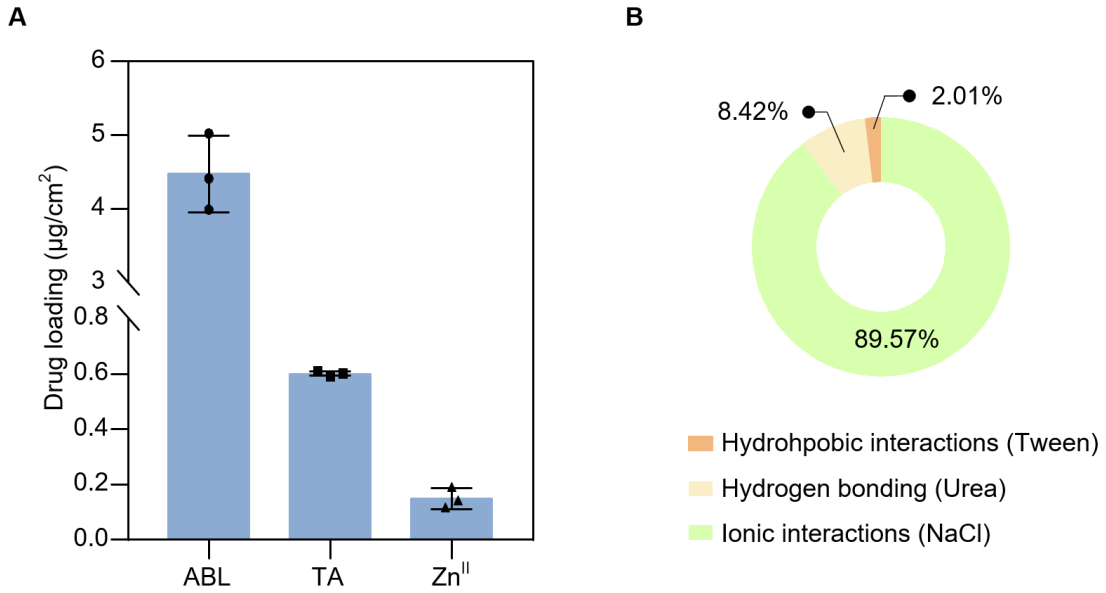

Fig. S1. (A) The loading efficiency of ABL, TA, and Zn^{II} in the ABL@ZnTA group. (B) Percentage of eluted ABL peptides based on interacting forces. The different colors note the ABL contents from different eluting solutions (100 mM urea, 100 mM Tween 20, or 100 mM NaCl), reflecting the interaction strength of ionic interactions, hydrogen bonding, and hydrophobic interactions, respectively.

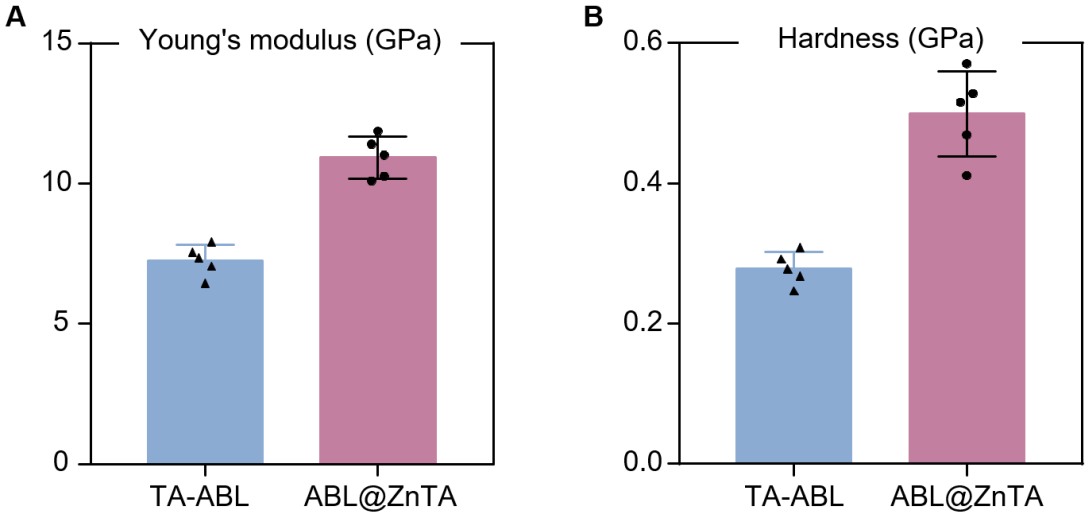

Fig. S2. Results of Young's modulus (A) and hardness (B) by nanoindentation.

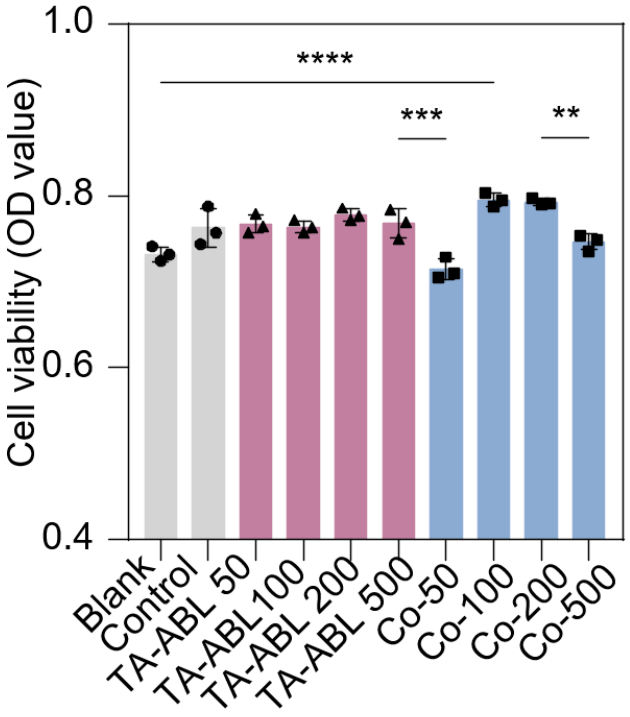

Fig. S3. CCK-8 results of macrophages on functional coatings of different concentrations at 2 days. The concentrations of TA-ABL 50 and Co-50 showed satisfactory properties and were used in the following experiments. Data are presented as mean ± SD. Statistical significance was calculated *via* one-way ANOVA with Tukey *posthoc* test (**, $P < 0.01$;*** $P < 0.001$; and ****, $P < 0.0001$).

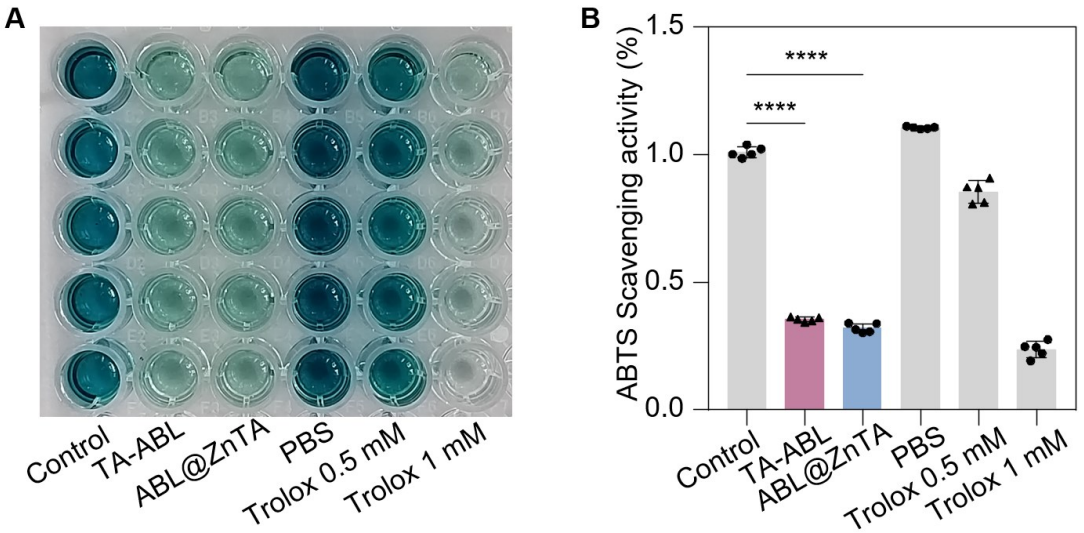

Fig. S4. ABTS scavenging properties of extracellular ROS level. (A) Image of the effect of various coatings on the scavenging of ABTS free radicals (blue color). (B) ABTS Scavenging activity (%) of functional coatings for microenvironmental ROS at 1 day. Data are presented as mean ± SD. Statistical significance was calculated *via* one-way ANOVA with Tukey *posthoc* test (****, $P < 0.0001$).

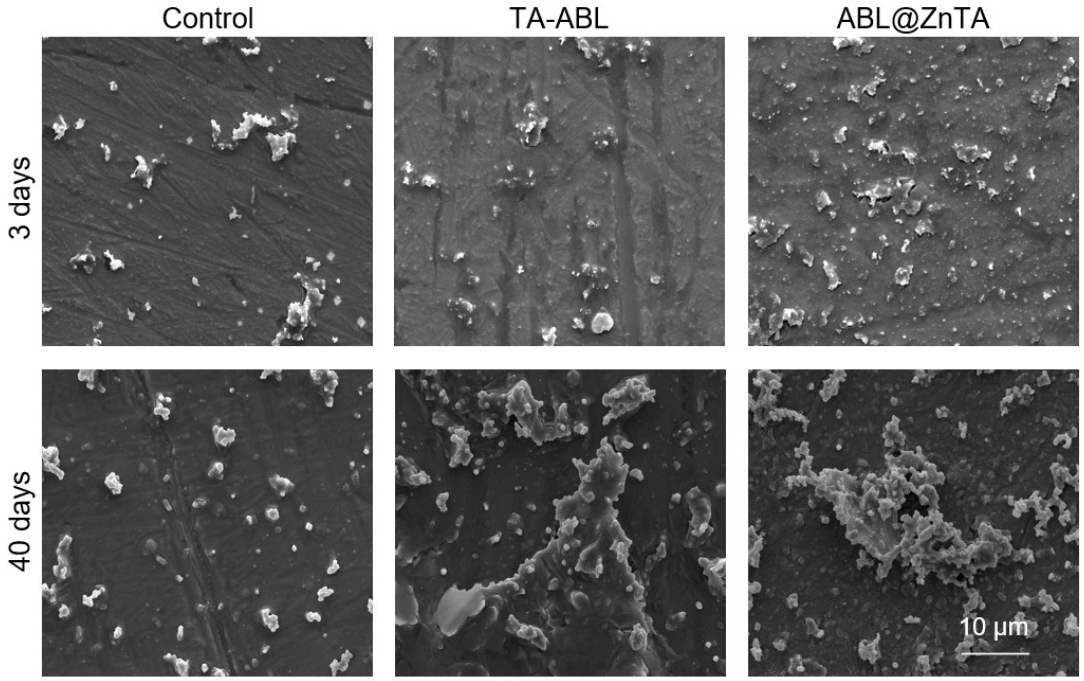

Fig. S5. SEM result of surface morphology of the samples in simulated body fluid for 3 and 40 days.

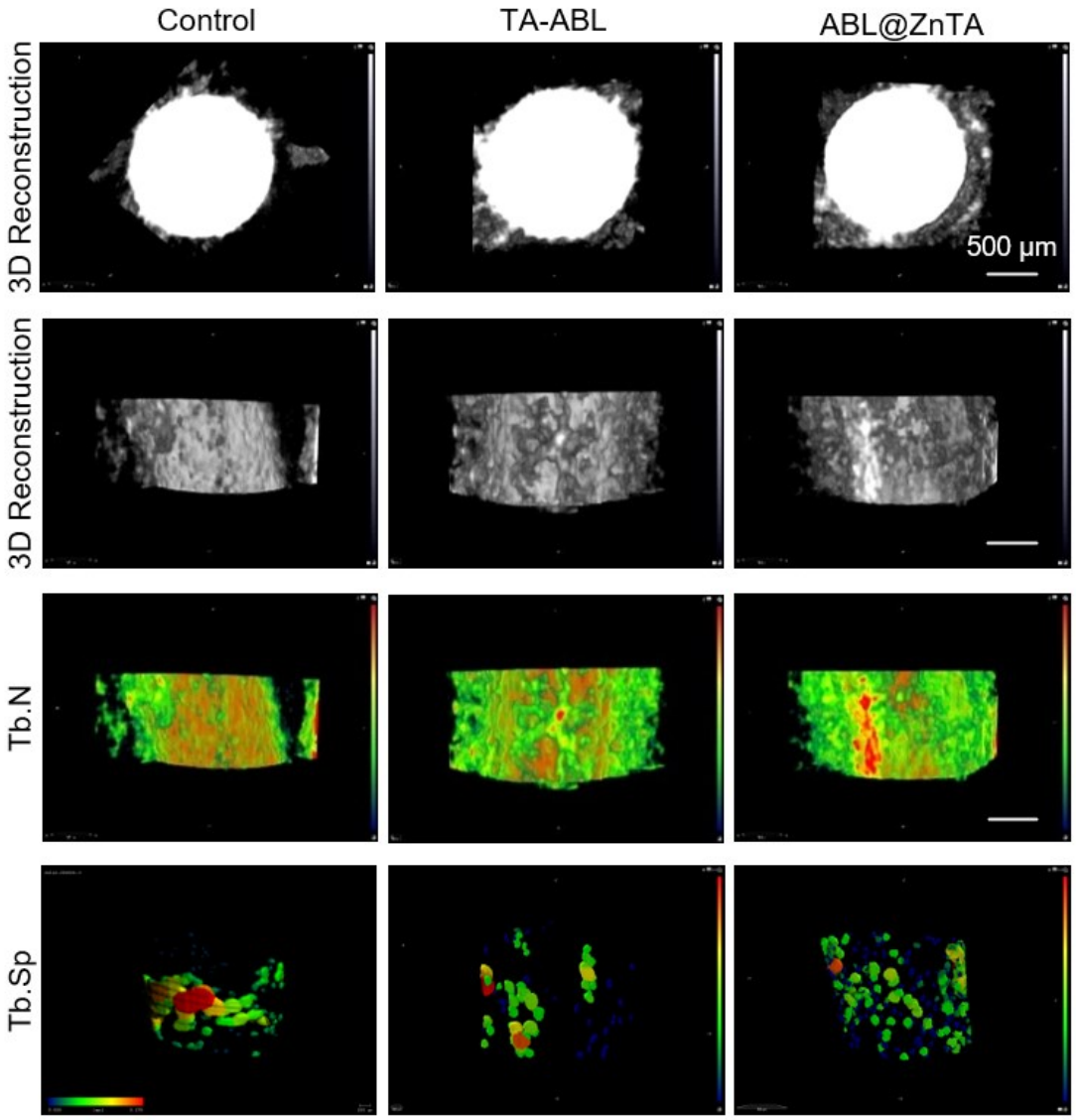

Fig. S6. Representative images of the 3D reconstructed Micro-CT images, Tb. N, and Tb. Sp of newborn bone at 28 days. Osseointegration strength and new bone formation around the implant are enhanced in the long term.

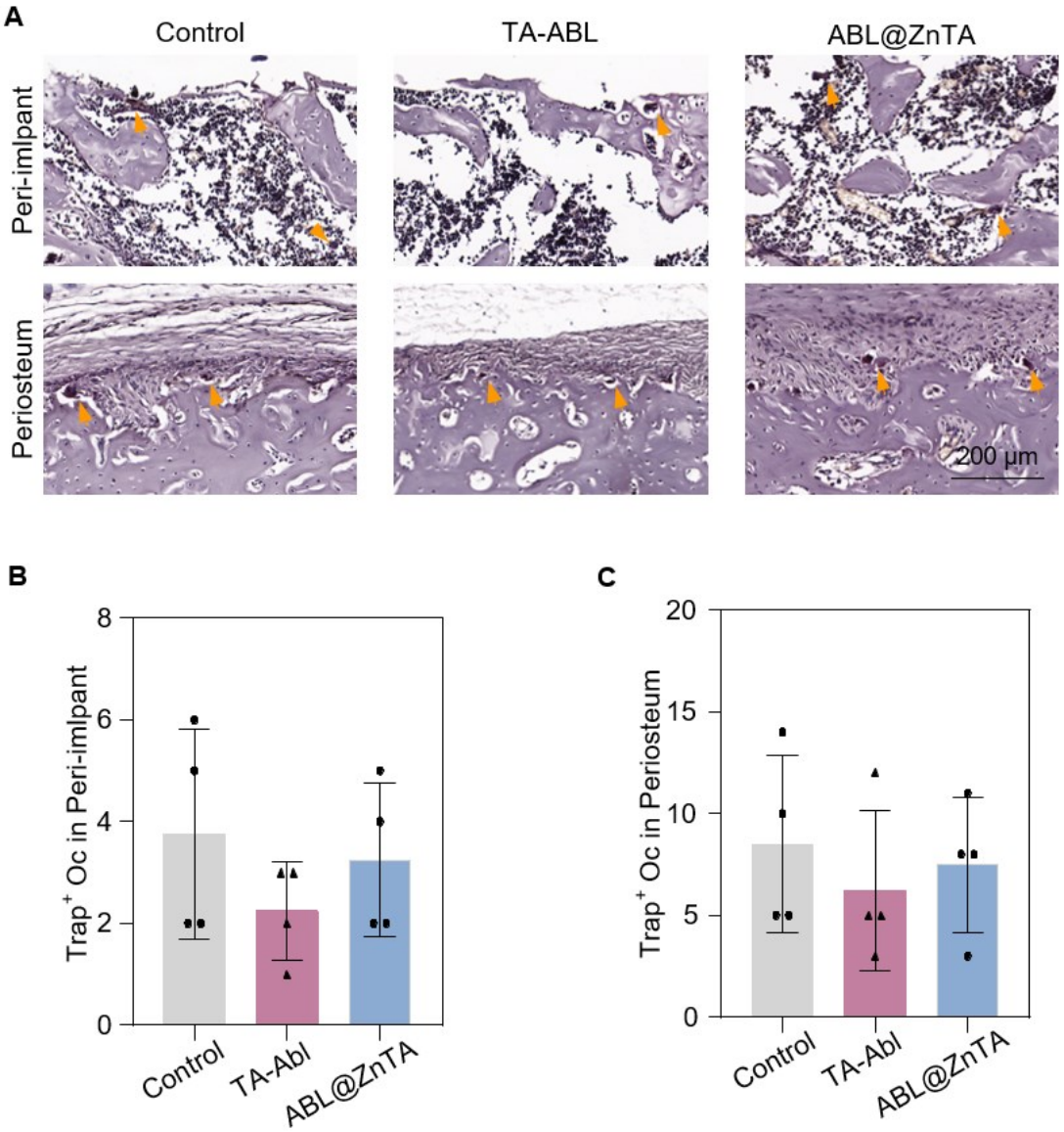

Fig. S7. Evaluation of osteoclastic differentiation of peri-implant. (A) Tartrate-resistant acid phosphatase (TRAP) staining in the peri-implant and nearby periosteum. (B) and (C) Semi-quantitative analysis of $Trap^+$ osteoclast numbers. Arrows indicate the osteoclasts (stained red), n = 4. Data are presented as mean ± SD. Statistical significance was calculated *via* one-way ANOVA with Tukey *posthoc* test. No statistical difference exists.

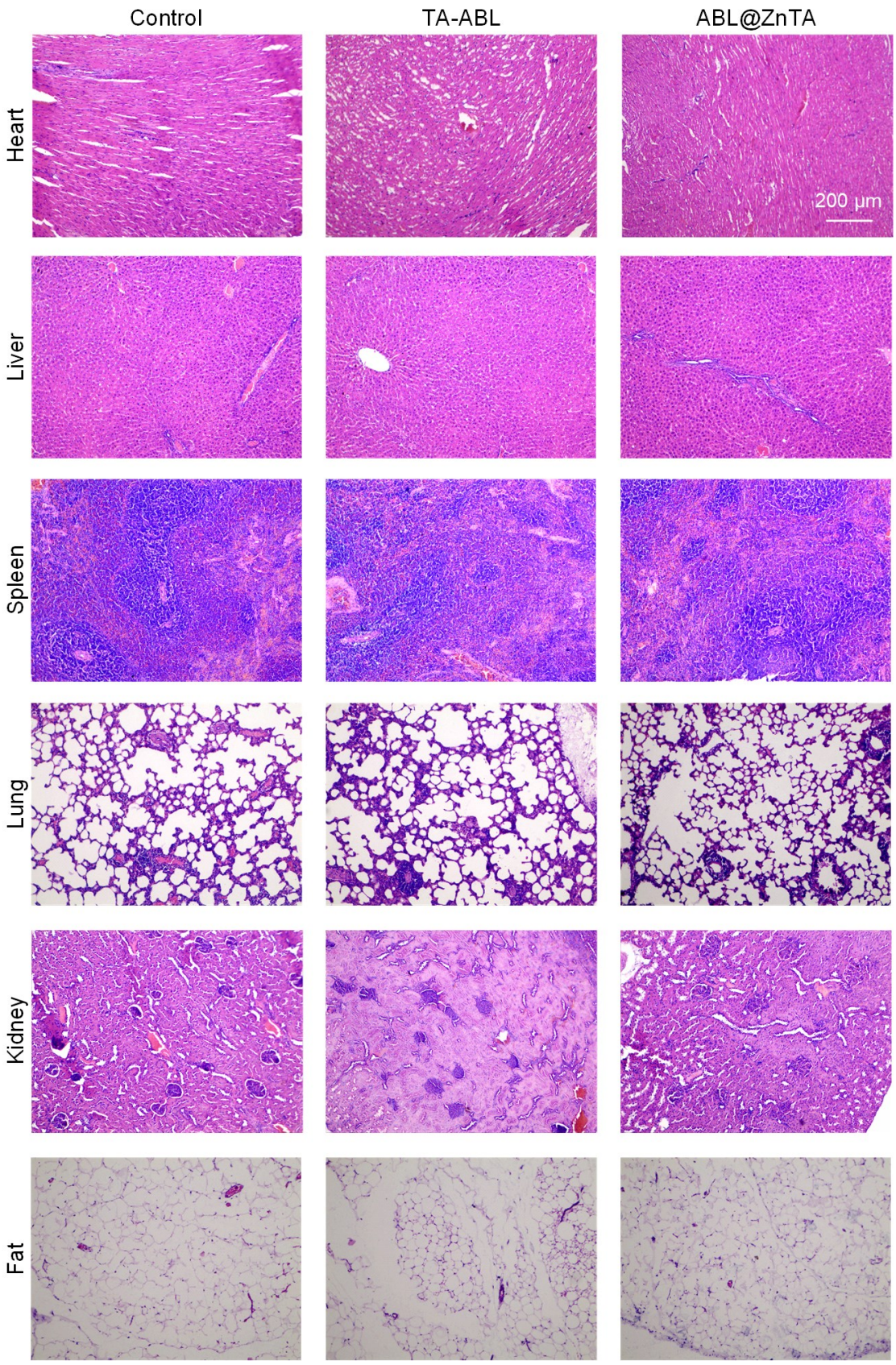

Fig. S8. Representative images of H&E staining of major organs at 28 days. No pathological changes were observed in the TA-ABL and ABL@ZnTA groups.

Reference

[1] H. Wang, X. Fu, J. Shi, et al., Nutrient element decorated polyetheretherketone implants steer mitochondrial dynamics for boosted diabetic osseointegration, Adv. Sci. 8(20) (2021) e2101778.